


Coverage-dependent electronic and optical properties of H- or F-passivated Si/Ag(111) from first principles

A. Ugolotti * and G. P. Brivio

Materials Science Department, Università degli Studi di Milano-Bicocca, via Cozzi 55, 20125 Milano, Italy

Guido Fratesi 

ETSF and Dipartimento di Fisica “Aldo Pontremoli,” Università degli Studi di Milano, via Celoria 16, 20133 Milano, Italy



(Received 24 December 2019; revised manuscript received 13 March 2020; accepted 14 April 2020; published 7 May 2020)

Chemical functionalization of silicene can be devised to tune the intrinsic properties for optoelectronic applications of this material, as well as for optimizing the interface formed by ultrathin Si and a substrate. This work is focused on the $(2\sqrt{3}\times 2\sqrt{3})R30^\circ$ phase of silicene grown on Ag(111), and the adsorption of H or F atoms, at half and full coverage, is simulated within density functional theory. The optical response is constructed through the independent particle–random-phase approximation and analyzed thoroughly. The connection between the electronic structure and the features in the optical absorption and reflection is therefore investigated in order to highlight either the role of the adatoms or the effect of the metallic surface. As the coverage is increased, the silicene phases are effectively decoupled from Ag by H or F adatoms and the freestanding properties of the corresponding systems are recovered, for which a coverage-dependent band gap is opened in the states of the overlayer. However, despite being effectively decoupled from the substrate, the properties of functionalized silicene do not show the peculiar characteristics expected from the ideal freestanding Si layer.

DOI: [10.1103/PhysRevB.101.195413](https://doi.org/10.1103/PhysRevB.101.195413)

I. INTRODUCTION

After the discovery of graphene [1], the unveiling of some of its interesting properties, as for example the high charge-carrier mobility [1,2], the fundamental optical conductivity [3–5], or the opportunity to deal with topological states [5,6], started the search for similar materials. Such an impulse led to intense research for compounds sharing the atomically thin honeycomb structure within group-IV elements, so-called Xenex [7–9]. Among those, great interest has been attracted by silicene [10] which would potentially be more compatible in Si-based optoelectronic technology. In its freestanding (FS) configuration, several properties of silicene have been thoroughly investigated by first-principles methods: geometry and stability [11], electronic [11–13] and optical [14–16] properties, and quantum effects [17,18]. The synthesis of a honeycomb layer of Si retaining the desired properties is still debated. In fact, despite the large number of materials available as support for silicene growth [7], a characteristic fingerprint of a two-dimensional honeycomb arrangement has not been unequivocally detected in experiments, despite promising results for silicene grown on dielectric surfaces [19,20].

Focusing on the Ag(111) surface, which is among the first and most investigated ones, scanning tunneling microscopy along with low-energy electron diffraction (LEED) [21–23],

Raman [24–26] and x-ray photoemission spectroscopy (XPS) [27] results suggest indeed the assembly of Si atoms into a continuous silicene sheet, although into several phases [28]. However, looking into the electronic properties it is possible to evince that Si atoms interact strongly with the substrate, by showing charge transfer effects [27] in XPS and a non-trivial hybridization of states in the band structure [22,29–32] by experimental and simulated angle-resolved photoemission spectroscopy (ARPES). Concerning optical spectra, a strong Si-Ag interaction has been further validated by experimental and theoretical studies [33,34].

In this picture, further chemical functionalization of silicene would help to investigate the nature of its interaction with a substrate, but also how its properties could be tuned for the fabrication of a device. Among the simplest modifications, the adsorption of single H or F atoms has been widely investigated from first-principles methods in the FS case [35–41] and hydrogenated bilayer silicene proposed for optoelectronic applications [42]. More recently, silicene quantum dots embedded in silicene have been studied for nanoscale magnetism [43]. These studies have addressed several absorption configurations at different coverage. For silicene epitaxially grown onto Ag(111), hydrogenation was investigated for structures up to 1:2 (H:Si) ratio, named half-silicene, where the adatoms decorate only one side of the Si monolayer [44–47]. The formation of a stable phase has been observed, where the adatoms stabilize the buckling of Si atoms into more regular patterns, paving the way to an ordered platform to further processing [48]. The interaction

*a.ugolotti@campus.unimib.it

of silicene grown on Ag(111) with F adatoms, among other cases, has been investigated at the level of electronic structures in Ref. [49], although for a different phase, the (4×4) one and a lower coverage. However, to the best of our knowledge, no study reports the properties of full epitaxial silicene (1:1 ratio) or the corresponding fluorinated cases, half-fluoro-silicene and fluoro-silicene, respectively.

Various phases are formed by silicene on Ag(111), e.g., as reported in Ref. [50] and further analyzed by LEED and ARPES in Ref. [29]. In this work we focus on the $(\sqrt{7}\times\sqrt{7})/(2\sqrt{3}\times 2\sqrt{3})R30^\circ$ reconstruction. Indeed, such a phase has been proved as a competitive one with respect to the (4×4) phase [51,52] and it has also been prepared as a pure phase not coexisting with other reconstructions [24,53]. Additionally, it has been shown to form an ordered half-silicene overlayer [45], whereas the (4×4) yields a 7:18 stoichiometry with lower symmetry [44]. Starting from the pristine silicene, we consider its functionalization through H or F atoms at half or full coverage, corresponding to a stoichiometric ratio between Si and the adatoms of 2:1 and 1:1, respectively. We investigate the geometric and electronic properties in the ground state, and simulate the dielectric response in relation to optical spectroscopies: absorption and surface differential reflectance spectra (SDRS). An in-depth analysis of the effect of the interaction at the interface on the electronic states at the surface, and their contribution to the dielectric response, is also provided.

II. METHODS

We calculated the ground-state geometry and the electronic wave functions through the density functional theory (DFT) framework [54,55], using a generalized gradient approximation with Perdew-Burke-Ernzerhof [56] exchange-correlation functional. We accounted for the van der Waals interaction by adding a pairwise force component in the form of the Grimme-D2 term [57] everywhere but Ag-Ag pairs. We enforced periodic boundary conditions and a plane-waves basis set as implemented in the QUANTUM ESPRESSO suite [58,59]. Norm-conserving, scalar-relativistic pseudopotentials have been employed, with a kinetic energy cutoff of 86 Ry. We obtain an Ag lattice constant $a_0 = 4.164 \text{ \AA}$ by fitting the bulk energy-volume curve and construct an asymmetric slab with five Ag layers, with the topmost two left free to relax. We included a vacuum region of at least 14.5 Å to minimize the interaction of the system with its replicas along the direction perpendicular to the surface. We sampled the two-dimensional reciprocal space of the surface supercell with an unshifted $6\times 6\times 1$ k -point mesh [60], increased to $17\times 17\times 1$ ($31\times 31\times 1$ for the FS cases) for calculating the electronic and the optical properties. The slabs at all coverages have been constructed with H and F atoms starting in the chairlike arrangement, which is among the most stable configuration for the free-standing case [36,37]. Moreover, such configuration is that already observed during the growth of hydrogenated silicene on Ag(111) [44,45,47].

The calculated wave functions have been therefore processed using the YAMBO code [61] to extract the macroscopic dielectric function ϵ_M . With the aim of simulating optical excitations at normal incidence, we chose to work within the

independent-particle random-phase approximation (IP-RPA), as previously validated in literature for either metallic [34] or insulating substrates [20]. In this case, assuming atomic units, the formula for the dielectric function reads [62]

$$\epsilon_M(\omega) = 1 + \frac{16\pi}{\Omega} \sum_{c,v,\mathbf{k}} \frac{W_{c\mathbf{k}}W_{v\mathbf{k}}}{\epsilon_{c\mathbf{k}} - \epsilon_{v\mathbf{k}}} \times \frac{|\langle v\mathbf{k}|\mathbf{p} + i[\mathbf{r}, V_{\text{NL}}]|c\mathbf{k}\rangle|^2}{(\epsilon_{c\mathbf{k}} - \epsilon_{v\mathbf{k}})^2 - (\omega + i\gamma)^2} \quad (1)$$

where Ω is the volume of the supercell, \mathbf{p} is the momentum operator, V_{NL} is the nonlocal term of the pseudopotential, and the $\epsilon_{l\mathbf{k}}$ are the Kohn-Sham (KS) eigenvalues. The IP-RPA approximation further allows us to separate valence and conduction band contributions localized on different atoms by including the relative weights $W_{l\mathbf{k}}$ of KS eigenstates $l\mathbf{k}$ over specific system portions [33]. To calculate the dielectric function, we restricted the cutoff for the plane-waves basis to 44 Ry.

For additional investigation of the contributions from pairs of valence-conduction state transitions to optical properties at a given energy ω , we sum the transition dipole moments (extracted from the YAMBO code) corresponding to the condition $\epsilon_{cv\mathbf{k}} \equiv \epsilon_{c\mathbf{k}} - \epsilon_{v\mathbf{k}} \in (\omega - \sigma, \omega + \sigma)$, where σ defines the width of a small allowed energy range around ω . Therefore we define the spectral intensity from states at energy E to transitions having energy $\approx \omega$ as

$$S(E, \omega) = \int_{\omega-\sigma}^{\omega+\sigma} d\omega' \sum_{v,c,\mathbf{k}} W_{v\mathbf{k}}W_{c\mathbf{k}}w_{\mathbf{k}}|\langle c\mathbf{k}|\hat{\mathbf{r}}|v\mathbf{k}\rangle|^2 \delta(\epsilon_{cv\mathbf{k}} - \omega') \times [\delta(\epsilon_{v\mathbf{k}} - E)\Theta(E_F - E) + \delta(\epsilon_{c\mathbf{k}} - E) \times \Theta(E - E_F)]. \quad (2)$$

Here, $w_{\mathbf{k}}$ is the weight of a k point, E_F is the Fermi energy, and the Dirac- δ are for computational purposes replaced by Gaussian functions. Besides these technicalities, $S(E, \omega)$ gives the electron-energy resolution of the imaginary part of ϵ_M :

$$\text{Im } \epsilon_M(\omega) \approx \int dE S(E, \omega). \quad (3)$$

The normal-incidence absorbance of a two-dimensional system can be written as [63]

$$\mathcal{A}(\omega) = \frac{\omega L}{c} \text{Im } \epsilon_M(\omega), \quad (4)$$

where L is the extension of the supercell orthogonal to the surface (here, 30 Å). For the SDRS, instead, we adopted a three-regions approach [64], in order to include the bulk response and to neglect the intraband component inside the response of the slab systems. Within this approximation, the differential reflectivity reads

$$\text{SDRS}(\omega) = \frac{4\omega L}{c} [A\Delta\epsilon'' - B\Delta\epsilon'], \quad (5)$$

$$A = \frac{\epsilon'_{\text{bulk}} - 1}{(1 - \epsilon'_{\text{bulk}})^2 + (\epsilon''_{\text{bulk}})^2}, \quad (6)$$

$$B = \frac{\epsilon''_{\text{bulk}}}{(1 - \epsilon'_{\text{bulk}})^2 + (\epsilon''_{\text{bulk}})^2}, \quad (7)$$

$$\Delta\epsilon = \epsilon_{\text{ads}} - \epsilon_{\text{clean}}, \quad (8)$$

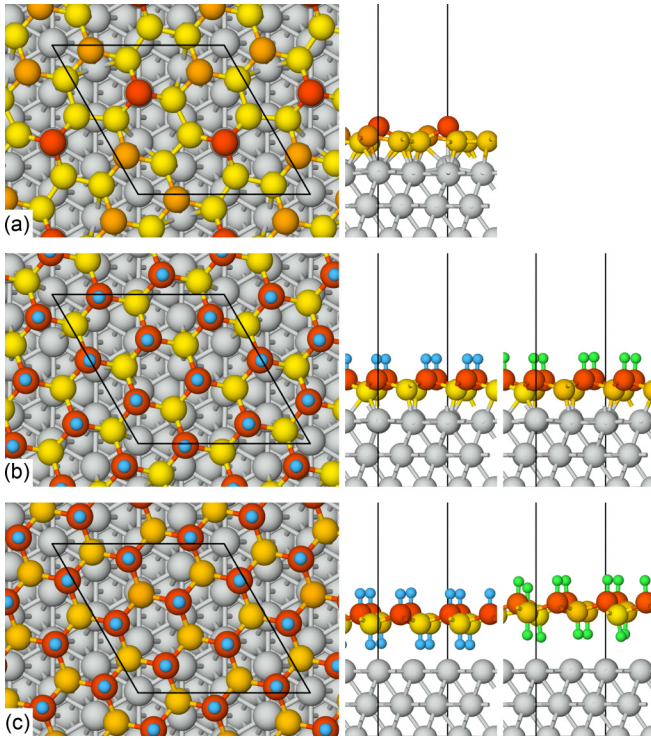


FIG. 1. Top (left) and front (right) views of relaxed silicene phases on Ag(111): (a) silicene (Si); (b) half-silicane (hSiH); (c) silicane (SiH). The front view is reported also for fluorinated phases (hSiF and SiF) in panels (b) and (c). Gray atoms: Ag; blue: H; green: F. The Si atoms are colored with a yellow-to-orange scale, depending on the height from the surface: the lower the atoms, the lighter the color. The black line depicts the border of the supercell.

where A and B are two weighting functions, which account for the response of bulk Ag, ϵ_{bulk} . For the calculation of ϵ_{bulk} only, we included the contribution of intraband transitions by manually adding a Drude pole at $h\nu = 8.90$ eV as obtained by the fitting of the experimental dielectric function [65].

III. RESULTS

Geometry. We report in Fig. 1 the relaxed configurations of the investigated phases on Ag(111), namely, silicene (Si), half-silicane (hSiH), silicane (SiH), half-fluorosilicane (hSiF), and fluorosilicane (SiF). Detailed geometrical parameters are collected in Table I, reporting the buckling b_{Si} of the Si layer, the Si-Si average bond lengths $d_{\text{Si-Si}}$, or the interlayer spacings between the various species, Δz_{X-Y} . The geometries of silicene and half-silicane are qualitatively in good agreement with the reference ones available from literature [24,47]. In visually comparing silicane to hSiH, intercalating further H atoms at the interface allows for the relaxation of Si atoms into a more regular arrangement, apparently less coupled with the Ag surface. The geometry for fluorinated phases is qualitatively similar to that of hydrogenated ones, with an increased interlayer distance upon fluorination. In all cases, the addition of H or F adatoms reduces the buckling of the Si layer. The interlayer distances, at all coverages, suggest a mixed chemical-physical adsorption character of

TABLE I. Geometric and energy details for the investigated silicene phases grown on Ag(111). Energies E are reported in eV per Si atom, interatomic distances Δz or bond lengths d and buckling b_{Si} in Å. X_u/X_d label the H or F passivating atoms adsorbed on the upper/lower face of the silicene sheet.

	Si	hSiH	SiH	hSiF	SiF
E_{ads} (eV/Si)	-0.70	-0.95	-0.17	-1.03	-0.19
$d_{\text{Si-Si}}$	2.32	2.36	2.34	2.36	2.35
$\Delta z_{\text{Si-Ag}}$	2.47	2.69	3.85	2.65	4.58
$\Delta z_{X_u\text{-Si}}$		1.90	1.85	2.00	1.97
$\Delta z_{\text{Si-}X_d}$			1.86		1.97
$\Delta z_{X_d\text{-Ag}}$			1.98		2.61
b_{Si}	1.15	0.89	0.79	0.98	1.01

the interaction. However, the positive trend observed for Si-Ag distances with increasing passivation already suggests an increased decoupling of the two subsystems.

Concerning the energetics, we compute the adsorption energy per Si atom $E_{\text{ads}}/\text{Si} = (E_{\text{SiXAg}} - E_{\text{SiX}} - E_{\text{Ag}})/N_{\text{Si}}$, where E_{SiX} is the total energy of the chosen coverage-dependent, passivated phase of silicene, E_{Ag} that of the Ag slab, and E_{SiXAg} that of the full system. As reported in Table I, all overlayers are favorably adsorbed onto the silver surface, with half-coverage phases being the most stable ones. The magnitude of binding energy, however, is sensibly smaller for higher-coverage silicenes, independently from the chemical species of the adatoms, which is a further indication of weaker interactions at the interface.

Electronic properties. The electronic band structures of the silicene phases investigated are collected in Fig. 2. The bands are projected on the atomic orbitals and colored according to the weight on the overlayer atoms (Si and possibly H/F). For silicene and half-silicane, the results are in good agreement with those already reported in literature [46,47]. For silicene/Ag(111) the contribution of Si orbitals is spread in energy at all points of the Brillouin zone, as expected from a strongly interacting system and the literature [29]. Progressively adding H or F, the projected bands indicate a larger separation between overlayer and Ag states, hence a smaller hybridization. This finding also facilitates the comparison with FS cases, reported in Fig. S1 of the Supplemental Material [66], especially for the fully hydrogenated/fluorinated cases.

The corresponding density of states (DOS) of the systems are shown in Fig. 3. Again, for silicene and half-silicene/Ag(111), these results are in good agreement with those already available in literature [29,47]. Looking to the DOS projected on Si orbitals, the phases with H/F at half coverage appear like poorly conducting metals with reduced DOS around the Fermi energy, while full-coverage phases show semiconducting band gaps amounting to ≈ 2 eV in silicane/Ag(111) and ≈ 0.5 eV in fluorosilicane. In all energy ranges, the Ag states dominate the DOS especially below -3 eV in correspondence to the Ag d band.

To visualize electron transfer occurring at the interface, we calculate the change in the real-space electron density of the full system with respect to that of the

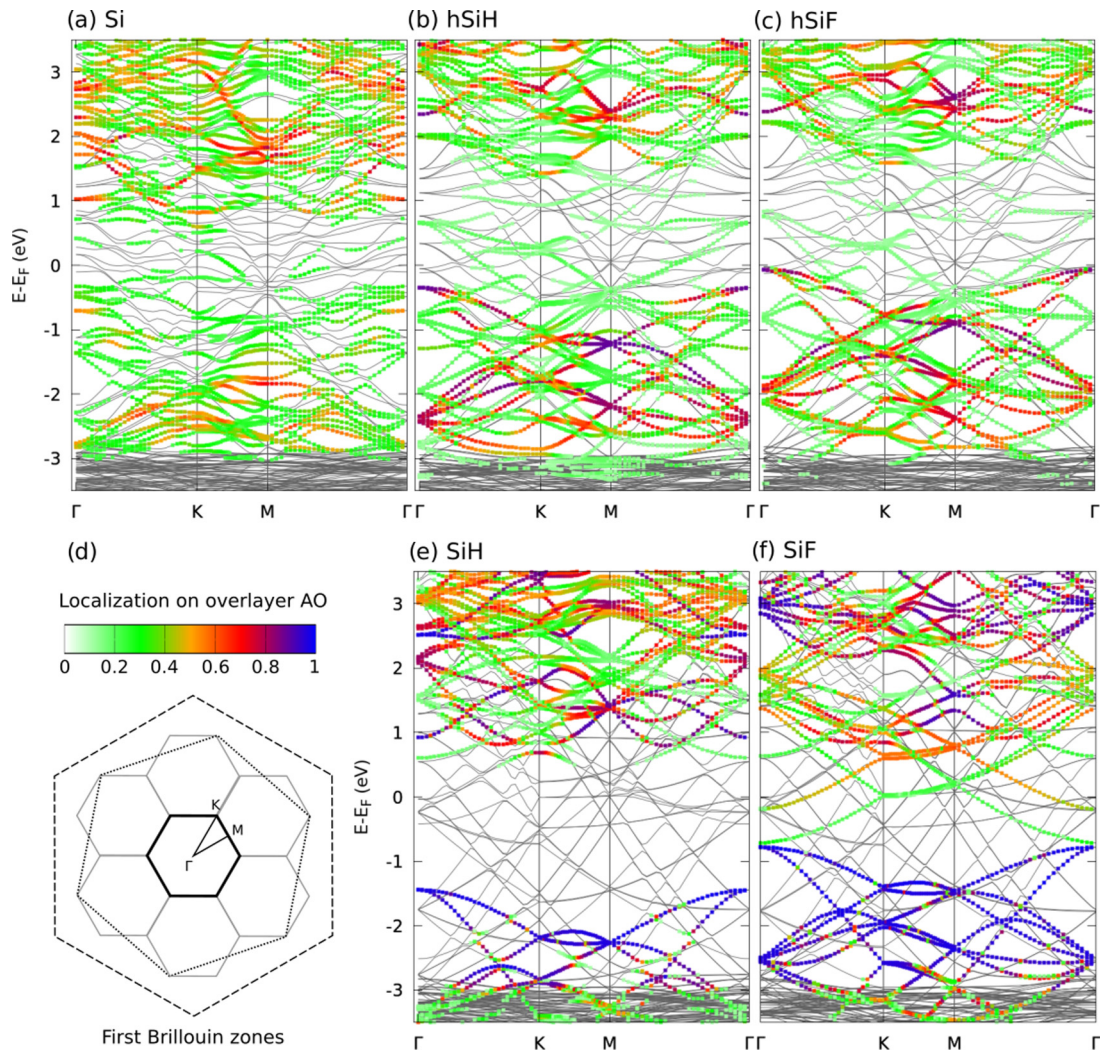


FIG. 2. Band structures (gray lines) for the silicene phases on Ag(111). The colored dots report, with a color scale from white-green to red-blue [shown in panel (d)], the weight of the projections of the system's wave functions onto the atomic orbitals (AO) of the respective overlayer. In panel (d) the Brillouin zones of the different systems are drawn: the (1×1) Ag(111), dashed line; the (1×1) silicene, dotted line; and the $(2\sqrt{3} \times 2\sqrt{3})$ supercell, solid lines; along with the high-symmetry points.

Ag(111) slab and of the peeled-off silicene phase, i.e., $\Delta n(\mathbf{r}) = n_{\text{SiH/Ag}}(\mathbf{r}) - n_{\text{Ag}}(\mathbf{r}) - n_{\text{SiH}}(\mathbf{r})$. The result is collected for all the systems in Fig. 4. Clearly the lobes of such density rearrangements are mainly located between the Si layer and the first Ag one. Especially the electron density accumulation visible for Si, hSiH, and hSiF in panels (a), (b), and (d), respectively, suggests the formation of bonds between Si and Ag. These bonds are weakened in the fully hydrogenated/fluorinated SiH/SiF phases [see panels (c)/(e)], where still some migration of electron density from Si and Ag layers to the center H/F atoms appears. We mention that, given the positioning of charge displacements in between the atoms, a partitioning over specific atoms may become misleading, as discussed in the Supplemental Material [66] where a table with Löwdin charges [67] is reported for completeness.

Optical properties. We investigate the optical excitations by constructing first the absorption spectra; the results are collected in Fig. 5 where we disentangle the contributions from the different chemical species. Three interesting energy ranges can be identified: a first one in the infrared, below 1 eV;

a second one in the visible range around 2.5–4.5 eV; and a third one in the ultraviolet above 5 eV. A correct analysis in the infrared range requires considering intraband transitions, giving rise to Drude peaks in metals, and exceedingly dense k -point meshes to correctly sample the Brillouin zone in the overlayers [15]. As a consequence of band folding and broken translational symmetry in the Ag(111) surface unit cell due to interaction with the overlayer, a Drude-like peak is apparent in our results [see especially the case of silicene in panel (a)], even though our calculations do not consider intraband transitions. This effect is considerably smaller for SiH and SiF at full coverage, given the smaller interaction with the substrate. In comparison, the third range is characterized by a featureless spectrum, mainly due to Ag-related interband transitions as evidenced by the projections on Ag atoms in the same figure. The second range is the most interesting to our purposes as it contains the most prominent features in the spectra due to the overlayer: for silicene, half-silicene, and half-fluorosilicene there is a main broad peak, with an onset at 3 eV. This feature overlaps with the onset of absorption from

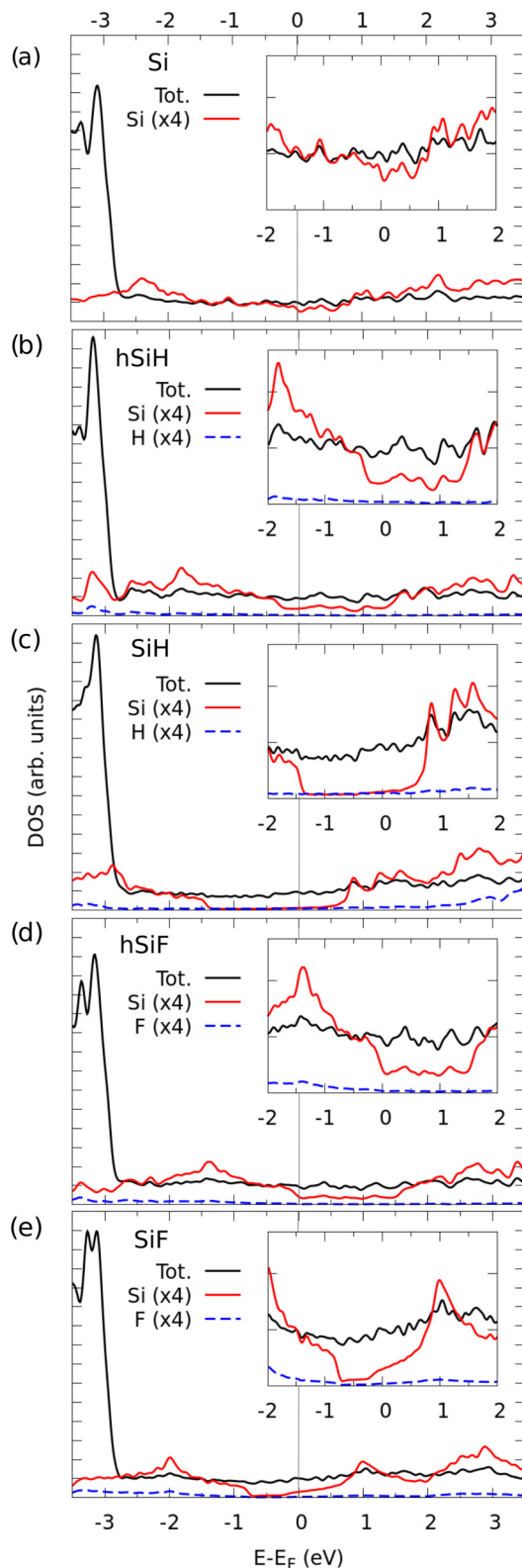


FIG. 3. DOS for the silicene phases on Ag(111) comparing the total system (black line) with the projection onto the Si (red line) and H/F (blue dashed line) atomic orbitals. The insets show a zoom around Fermi energy.

Ag(111) occurring at about the same energy [see Fig. S2(b) in the Supplemental Material [66] for results for the clean slab].

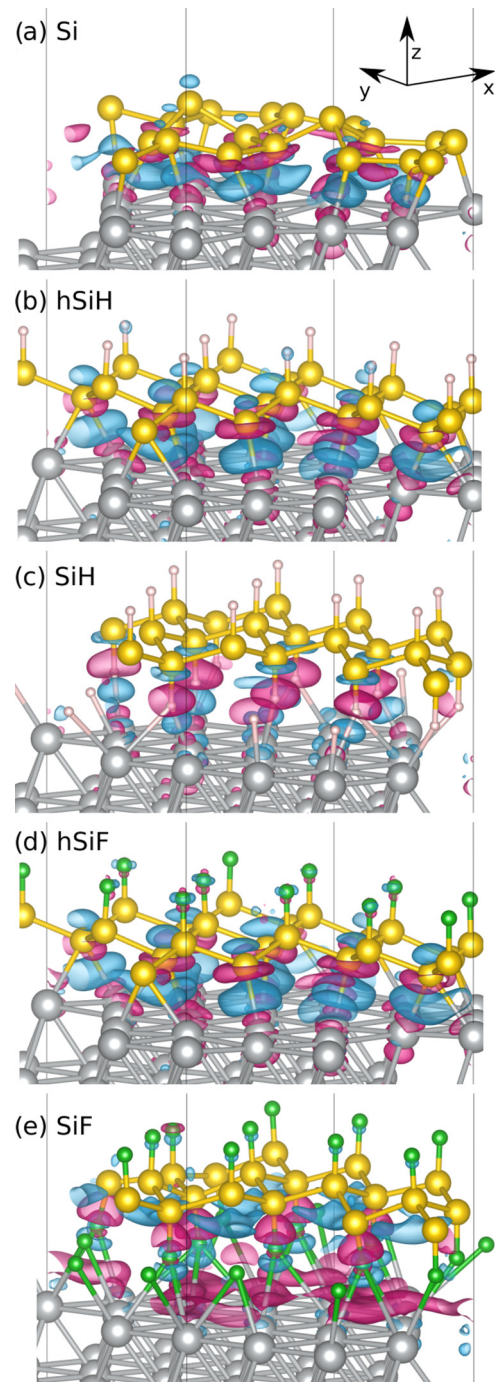


FIG. 4. Perspective views of electron density redistributions due to adsorption of the overlayer onto the surface, Δn , for silicene phases on Ag(111), for an isovalue of $0.001 e/\text{\AA}^3$. Magenta/cyan lobes indicate electron depletion/accumulation areas, respectively. Yellow atoms: Si; gray: Ag; white: H; green: F. The gray lines track the edges of each supercell.

The strong interaction at the interface seen in the band structure analysis manifests itself by the mixture of Ag contributions to Si-derived peaks, such as Si(valence)-Ag(conduction), Ag-Si, and Ag-Ag transitions, whose intensities are overwhelming. As the coverage increases, the Si-related component within the spectra becomes sharper and in closer resemblance to their FS counterpart (the

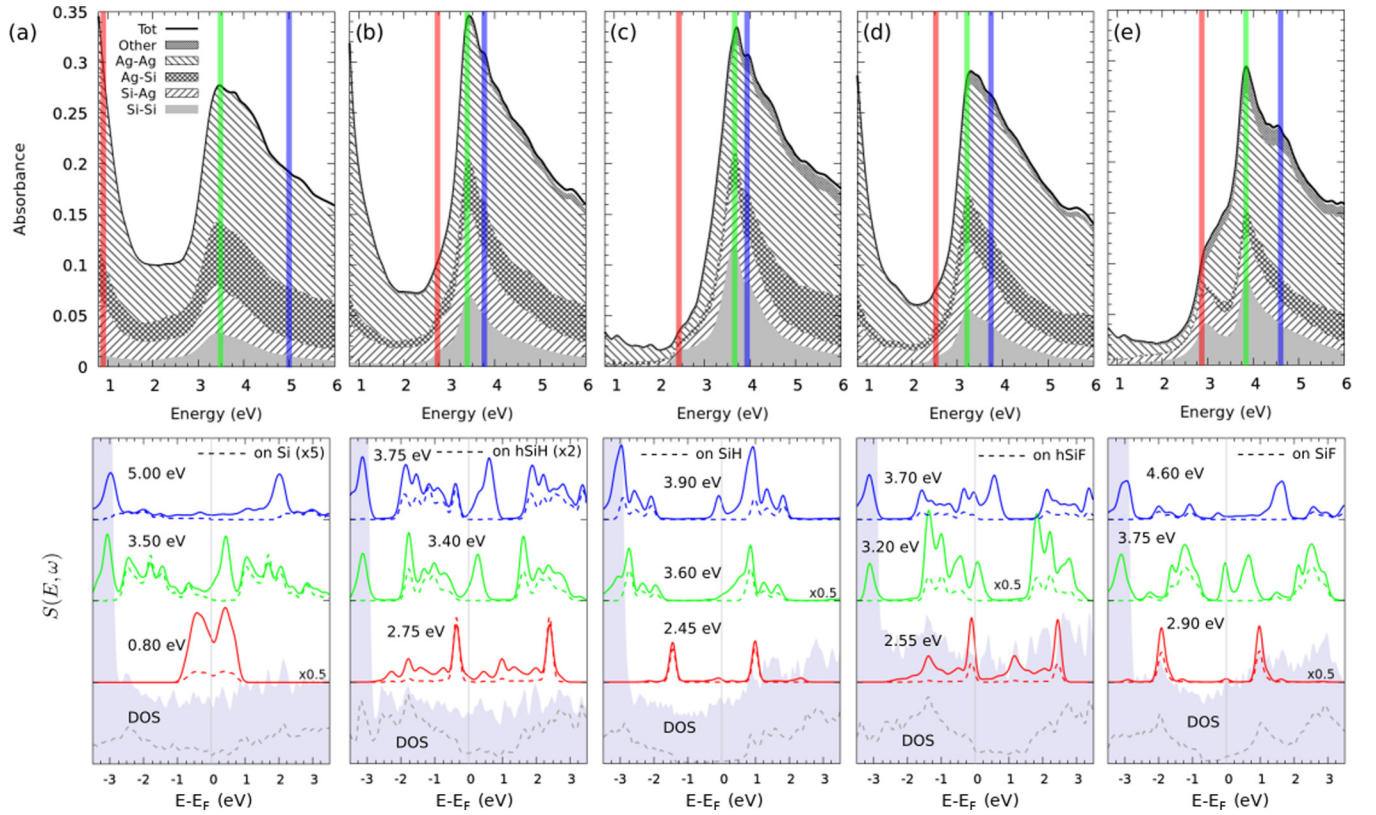


FIG. 5. Top panels: optical absorption spectra for (a) Si, (b) hSiH, (c) SiH, (d) hSiF, and (e) SiF on Ag(111), showing the different valence to conduction contributions. The transitions involving H or F atomic states are grouped under the label “Other”. Bottom panels: spectral intensities $S(E, \omega)$ for the transition energies ω reported close to each plot and marked within the absorbance spectra by the corresponding colors. For comparison, the DOS is shown with the gray area/lines. The features of the adsorbed systems are reported with solid lines, whereas their projections on the silicene overlayers are shown with dashed lines.

latter reported in Fig. S2 of the Supplemental Material [66]), suggesting a weaker interaction at the interface. The progressive decoupling of the overlayer from the surface as H/F coverage increases emerges by analyzing Si-Si components which become sharper and more intense with increasing hydrogenation/fluorination (see Fig. S5 in the Supplemental Material [66] for an easier comparison).

We further analyze the absorption spectra by identifying the valence and conduction states contributing to absorption at few specific energies. To do so, we evaluated the spectral intensity function, as described in Eq. (1). The result is reported in the right panels of Fig. 5 for transitions of interest in the interval $(\omega - \sigma, \omega + \sigma)$ as marked in the left panels with colored ranges, having chosen $\sigma = 0.05$ eV. The green line is at the main peak in the absorption spectrum, whereas red/blue lines are chosen at lower/higher energies, with values depending on the system of investigation. We report the total spectral intensity as well as the contribution by Si states only [extracted by using the projections on the atomic orbitals of the overlayers as the weights W_i in Eq. (2)]. In practice, the curves are peaked at the energy of valence and conduction states which have the highest transition dipole moments and therefore contribute most to absorption. Since, to the best of our knowledge, such an analysis has not been performed for the passivated phases of silicene, we briefly discuss the corresponding freestanding cases in the Supplemental Material [66].

For silicene grown on Ag(111), as reported in Fig. 5(a), the contribution of Si atoms is centered at ≈ 3.5 eV adding to the main spectral feature. As shown by the green dashed line, the electronic states involved in such transitions come from states that, especially for the conduction band, lie away from E_F . Such main component resembles that of FS silicene, although at little lower energy. When adsorbed on Ag(111), the absorption spectrum of silicene loses its characteristic peak at lower energies [≈ 1.65 eV in Fig. S2(a) of the Supplemental Material [66]], originated from the excitation from/to the band edges, as those states are participating in the formation of new bonds with Ag atoms. If we now look to the low-energy transitions of the Drude-like peak, both Si and Ag states contribute, although with different intensities.

For both hSiH and hSiF on Ag(111), reported in Figs. 5(b) and 5(d), respectively, the absorption spectra around 3.40 and 3.20 eV are a superposition of the transitions originated from the edge of the d band of Ag and those from the states of Si around the pseudo-band gap, where the projected DOS is strongly reduced. Such behavior is in agreement with that of the corresponding FS silicene phases, which are shown in Figs. S2(c) and S2(d) of the Supplemental Material [66]. An even better agreement between the optical spectrum of the FS and of the adsorbed layers can be observed at other energies (e.g., 2.75 and 2.55 eV, respectively), where the absorption can be more easily disentangled through the spectral intensity; this suggests already a weaker coupling at the interface

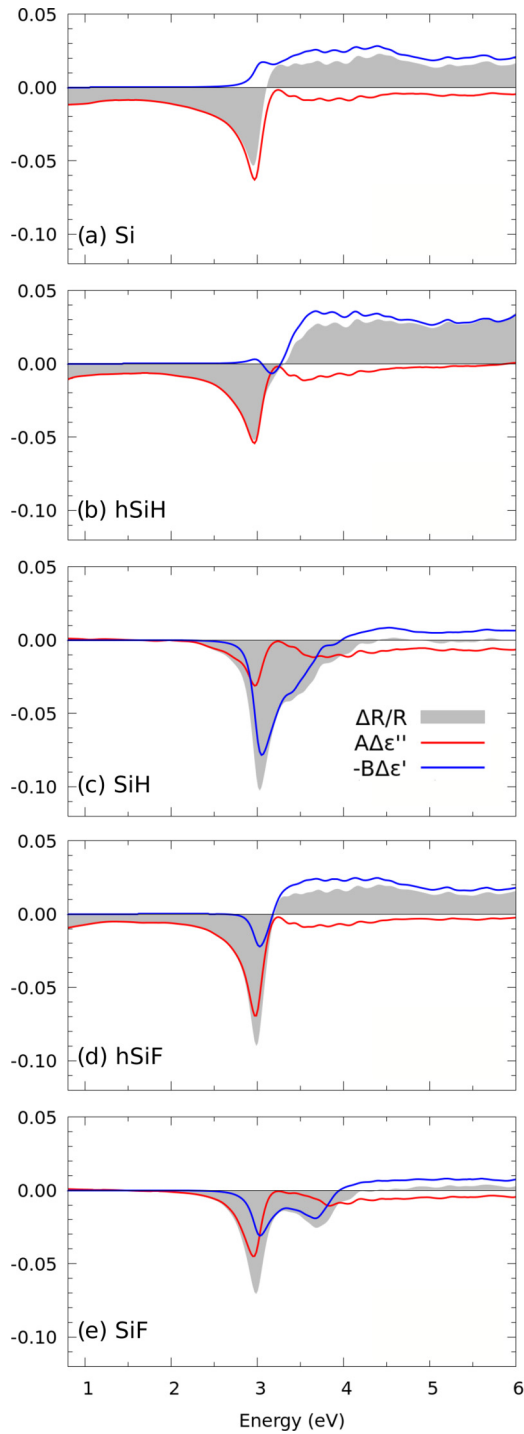


FIG. 6. Simulated SDRS spectrum for (a) Si, (b) hSiH, (c) SiH, (d) hSiF, and (e) SiF on Ag(111).

induced by the passivation of Si atoms. On the low-energy side of the main peak a small shoulder appears that anticipates a feature emerging for fully passivated systems discussed next.

In the case of SiH and SiF on Ag(111), the spectra reported in Figs. 5(c) and 5(e) show the formation of characteristic features at ≈ 3.60 and 3.70 eV, respectively. The spectral intensity for these systems well separates regions with negligible Si weight and ones where the Si-Si contribution instead strongly

resembles the pristine spectra reported in Figs. S5(b), S5(e), and S5(f) of the Supplemental Material [66]. This allows us to easily interpret some spectral features by comparison to FS ones. For example, the peak at ≈ 2.45 eV corresponds to the one at the same energy in the FS originated by transitions between band edges at Γ in the reciprocal space of SiH. Similarly, the one at ≈ 2.90 eV corresponds to a Van Hove singularity at the M points in the reciprocal space of FS SiF. These features, at lower intensity, are already visible in the corresponding half-coverage systems.

For all cases, we also report the analysis at energy larger than the main peak (blue lines) typically showing the addition of Ag contributions having valence states at the upper edge of the d band, with Si states in a wide energy range.

We finally investigate the systems by means of the changes in the reflectivity through SDRS data, which is collected in Fig. 6; as a reference, the reflectivity spectrum computed using Fresnel's equation with the bulk Ag response is reported in Fig. S4 of the Supplemental Material [66]. The results for silicene are in good agreement with the ones already reported in literature [34], even though for a different silicene/Ag phase, indicating a mild dependence of optical properties on the detailed silicene structure previously pointed out [33]. All SDRS spectra are characterized by large negative features around 3 eV, broader for silicene and fluorosilicene; this value corresponds, at least in our simulations, to the onset of optical absorption of both the adsorbate and Ag surface (more detail is given in the Supplemental Material [66]). For silicene and fluorosilicene, this is the only observable feature, which is characterized by a peak with a shoulder for SiH and a double peak for SiF (discussed in the next paragraph). Conversely, for lower adatom coverages, the reflectivity of the slab differs from that of the clean surface also at higher and lower energies.

We further address the SDRS by reporting separately the two terms related to the imaginary and real parts of $\Delta\epsilon$ summing up to the spectrum as in Eq. (5). The two weighting functions A, B we extracted are reported in the Supplemental Material [66] (Fig. S4). For silicene, hSiH, and hSiF, the SDRS spectrum is mainly characterized by an increased absorption ($\epsilon''_{\text{ads}} > \epsilon''_{\text{clean}}$) for energies below 3.2 eV, while for higher energies the SDRS spectra are due to $\epsilon'_{\text{ads}} < \epsilon'_{\text{clean}}$. For SiH and SiF, the total SDRS spectrum shows only a broad negative feature between 3 and 4 eV; investigating its components, as in the other cases, it is possible to observe the effect of the increased absorption which is related to the presence of an overlayer on top of the surface. For the fully passivated silicenes, however, the intensity of the real term of the dielectric function is more important.

IV. CONCLUSIONS

We have investigated the effects of passivating an epitaxially grown silicene monolayer on Ag(111) at different coverages by first-principles approaches. As prototypes of chemical functionalization, we considered adsorption of atomic H or F, at 1:2 and 1:1 ratios compared with Si atoms. We constructed the ground-state geometry of each system through DFT calculations and extracted the band structure and DOS.

We have investigated the fingerprints of the interaction at the interface, such as the decomposition of the electronic states onto the atomic orbitals of the silicene overlayers. We have observed that the effect of the passivating H or F adatoms is to weaken the coupling with the Ag surface, as the projected electronic structure increasingly resembles that of the corresponding FS case. In particular, this drives the transition of the functionalized silicene from a metal to a semiconductor, where the size of the band gap depends on the chemical species of the adatom. We investigated optical excitations and determined the dielectric function at the independent-particle level. We propose an analysis that allows one to reconnect spectral features with specific energy- and wave-vector-resolved electronic properties. With respect to the pristine silicene/Ag(111) case, the evolution of spectral components highlights a weakening interaction at the interface with increasing adatom coverage, as can be seen by a sharpening of silicene-related features indicating their increased localization on the overlayer. At full coverage, the absorption spectra clearly presents an additional component, at about 1 eV lower energy than the main peak. Our analysis aimed at the intensities of the transition dipole elements for the most characteristic transition energies. We have shown that the aforementioned component is indeed peculiar to the

FS functionalized silicene, although with a different origin: in FS silicene, it is a mild feature, originated from the valence-band maximum to conduction-band minimum transition of FS silicene. For fluorosilicene, it is instead a more pronounced shoulder that is reminiscent of a Van Hove singularity in the electronic structure of FS fluorosilicene. Looking for viable experimental characterization techniques, we computed the reflectivity, compared with that of the clean surface, as in the SDRS technique. We have been able to show that the degree of coverage can be effectively addressed as the different spectral shapes can be observed. Even though the reflectivity changes at ≈ 3 eV in all systems, its actual shape is different as silicene is fully passivated; in which case the measurement of the components of the dielectric function allows for discriminating the coverage step.

Overall, we have addressed several differences which distinguish passivation by H atoms from F atoms, which are reminiscent of the differences between free-standing monolayers. Hydrogenation and fluorination are effective in altering the properties of silicene/Ag(111) and in reducing the interaction at the interface. However, because of the reactivity of Si atoms, even the coupling with the passivating adatoms is strong enough to disrupt the Dirac structure, peculiar to that expected from the ideal freestanding silicene.

-
- [1] K. S. Novoselov, A. K. Geim, S. V. Morozov, D. Jiang, Y. Zhang, S. V. Dubonos, I. V. Grigorieva, and A. A. Firsov, Electric field effect in atomically thin carbon films, *Science* **306**, 666 (2001).
- [2] K. S. Novoselov, A. K. Geim, S. V. Morozov, D. Jiang, M. I. Katsnelson, I. V. Grigorieva, S. V. Dubonos, and A. A. Firsov, Two-dimensional gas of massless Dirac fermions in graphene, *Nature (London)* **438**, 197 (2005).
- [3] K. F. Mak, M. Y. Sfeir, Y. Wu, C. H. Lui, J. A. Misewich, and T. F. Heinz, Measurement of the Optical Conductivity of Graphene, *Phys. Rev. Lett.* **101**, 196405 (2008).
- [4] V. P. Gusynin and S. G. Sharapov, Transport of Dirac quasiparticles in graphene: Hall and optical conductivities, *Phys. Rev. B* **73**, 245411 (2006).
- [5] R. R. Nair, P. Blake, A. N. Grigorenko, K. S. Novoselov, T. J. Booth, T. Stauber, N. M. R. Peres, and A. K. Geim, Fine structure constant defines visual transparency of graphene, *Science* **320**, 1308 (2008).
- [6] Y. Zhang, Y.-W. Tan, H. L. Stormer, and P. Kim, Experimental observation of the quantum Hall effect and Berry's phase in graphene, *Nature (London)* **438**, 201 (2005).
- [7] A. Molle, J. Goldberger, M. Houssa, Y. Xu, S.-C. Zhang, and D. Akinwande, Buckled two-dimensional Xene sheets, *Nat. Mater.* **16**, 163 (2017).
- [8] L. C. Lew Yan Voon and G. G. Guzmán-Verri, Is silicene the next graphene?, *MRS Bull.* **39**, 366 (2014).
- [9] S. Cahangirov, H. Sahin, G. Le Lay, and A. Rubio, *Introduction to the Physics of Silicene and Other 2D Materials* (Springer International Publishing AG, Cham, Switzerland, 2017).
- [10] A. Kara, H. Enriquez, A. P. Seitsonen, L. C. Lew Yan Voon, S. Vizzini, B. Aufray, and H. Oughaddou, A review on silicene—New candidate for electronics, *Surf. Sci. Rep.* **67**, 1 (2012).
- [11] S. Cahangirov, M. Topsakal, E. Aktürk, H. Şahin, and S. Ciraci, Two- and One-Dimensional Honeycomb Structures of Silicon and Germanium, *Phys. Rev. Lett.* **102**, 236804 (2009).
- [12] R. Qin, C.-H. Wang, W. Zhu, and Y. Zhang, First-principles calculations of mechanical and electronic properties of silicene under strain, *AIP Adv.* **2**, 022159 (2012).
- [13] Z.-G. Shao, X.-S. Ye, L. Lei Yang, and C.-L. Wang, First-principles calculation of intrinsic carrier mobility of silicene, *J. Appl. Phys.* **114**, 093712 (2013).
- [14] L. Matthes, O. Pulci, and F. Bechstedt, Optical properties of two-dimensional honeycomb crystals graphene, silicene, germanene, and thiene from first principles, *New J. Phys.* **16**, 105007 (2014).
- [15] L. Matthes, P. Gori, O. Pulci, and F. Bechstedt, Universal infrared absorbance of two-dimensional honeycomb group-IV crystals, *Phys. Rev. B* **87**, 035438 (2013).
- [16] W. Wei and T. Jacob, Strong many-body effects in silicene-based structures, *Phys. Rev. B* **88**, 045203 (2013).
- [17] M. Ezawa, A topological insulator and helical zero mode in silicene under an inhomogeneous electric field, *New J. Phys.* **14**, 033003 (2012).
- [18] M. Ezawa, Valley-Polarized Metals and Quantum Anomalous Hall Effect in Silicene, *Phys. Rev. Lett.* **109**, 055502 (2012).
- [19] C. Grazianetti, S. De Rosa, C. Martella, P. Targa, D. Codegioni, P. Gori, O. Pulci, A. Molle, and S. Lupi, Optical conductivity of two-dimensional silicon: Evidence of Dirac electrodynamics, *Nano Lett.* **18**, 7124 (2018).
- [20] P. Gori, I. Kupchak, F. Bechstedt, D. Grassano, and O. Pulci, Honeycomb silicon on alumina: Massless Dirac fermions in silicene on substrate, *Phys. Rev. B* **100**, 245413 (2019).
- [21] B. Lalmi, H. Oughaddou, H. Enriquez, A. Kara, S. Vizzini, B. Ealet, and B. Aufray, Epitaxial growth of a silicene sheet, *Appl. Phys. Lett.* **97**, 223109 (2010).

- [22] P. Vogt, P. De Padova, C. Quaresima, J. Avila, E. Frantzeskakis, M. C. Asensio, A. Resta, B. Ealet, and G. Le Lay, Silicene: Compelling Experimental Evidence for Graphenelike Two-Dimensional Silicon, *Phys. Rev. Lett.* **108**, 155501 (2012).
- [23] C.-L. Lin, R. Arafune, K. Kawahara, N. Tsukahara, E. Minamitani, Y. Kim, N. Takagi, and M. Kawai, Structure of silicene grown on Ag(111), *Appl. Phys. Exp.* **5**, 045802 (2012).
- [24] E. Cinquanta, E. Scalise, D. Chiappe, C. Grazianetti, B. van den Broek, M. Houssa, M. Fanciulli, and A. Molle, Getting through the nature of silicene: An sp^2 - sp^3 two-dimensional silicon nanosheet, *J. Phys. Chem. C* **117**, 16719 (2013).
- [25] D. Solonenko, O. D. Gordan, G. Le Lay, H. Şahin, S. Cahangirov, D. R. T. Zahn, and P. Vogt, 2D vibrational properties of epitaxial silicene on Ag(111), *2D Mater.* **4**, 015008 (2016).
- [26] D. Solonenko, V. Dzhagan, S. Cahangirov, C. Bacaksiz, H. Sahin, D. R. T. Zahn, and P. Vogt, Hydrogen-induced sp^2 - sp^3 rehybridization in epitaxial silicene, *Phys. Rev. B* **96**, 235423 (2017).
- [27] A. Molle, C. Grazianetti, D. Chiappe, E. Cinquanta, E. Cianci, G. Tallarida, and M. Fanciulli, Hindering the oxidation of silicene with non-reactive encapsulation, *Adv. Funct. Mater.* **23**, 4340 (2013).
- [28] A. Curcella, R. Bernard, Y. Borenstein, A. Resta, M. Lazzeri, and G. Prévot, Structure and stability of silicene on Ag(111) reconstructions from grazing incidence x-ray diffraction and density functional theory, *Phys. Rev. B* **99**, 205411 (2019).
- [29] P. M. Sheverdyaeva, S. K. Mahatha, P. Moras, L. Petaccia, G. Fratesi, G. Onida, and C. Carbone, Electronic states of silicene allotropes on Ag(111), *ACS Nano* **11**, 975 (2017).
- [30] Y. Feng *et al.*, Direct evidence of interaction-induced Dirac cones in a monolayer silicene/Ag(111) system, *Proc. Natl. Acad. Sci. USA* **113**, 14656 (2016).
- [31] B. Feng, H. Zhou, Y. Feng, H. Liu, S. He, I. Matsuda, L. Chen, E. F. Schwier, K. Shimada, S. Meng, and K. Wu, Superstructure-Induced Splitting of Dirac Cones in Silicene, *Phys. Rev. Lett.* **122**, 196801 (2019).
- [32] S. Cahangirov, M. Audiffred, P. Tang, A. Iacomino, W. Duan, G. Merino, and A. Rubio, Electronic structure of silicene on Ag(111): Strong hybridization effects, *Phys. Rev. B* **88**, 035432 (2013).
- [33] E. Cinquanta, G. Fratesi, S. dal Conte, C. Grazianetti, F. Scotognella, S. Stagira, C. Vozzi, G. Onida, and A. Molle, Optical response and ultrafast carrier dynamics of silicene-silver interface, *Phys. Rev. B* **92**, 165427 (2015).
- [34] C. Hogan, O. Pulci, P. Gori, F. Bechstedt, D. S. Martin, E. E. Barritt, A. Curcella, G. Prevot, and Y. Borenstein, Optical properties of silicene, Si/Ag(111), and Si/Ag(110), *Phys. Rev. B* **97**, 195407 (2018).
- [35] H. Houssa, E. Scalise, K. Sankaran, G. Pourtois, V. V. Afans'ev, and A. Stesmans, Electronic properties of hydrogenated silicene and germanene, *Appl. Phys. Lett.* **98**, 223107 (2011).
- [36] Y. Ding and Y. Wang, Electronic structures of silicene fluoride and hydride, *Appl. Phys. Lett.* **100**, 083102 (2012).
- [37] P. Zhang, X. D. Li, C. H. Hu, S. Q. Wu, and Z. Z. Zhu, First-principles studies of the hydrogenation effects in silicene sheets, *Phys. Lett. A* **376**, 1230 (2012).
- [38] F. Zheng and C. Zhang, The electronic and magnetic properties of functionalized silicene: A first-principles study, *Nanoscale Res. Lett.* **7**, 422 (2012).
- [39] X. Wang, H. Liu, and S.-T. Tu, First-principles study of half-fluorinated silicene sheets, *RCS Adv.* **5**, 6238 (2015).
- [40] M. Pizzochero, M. Bonfanti, and R. Martinazzo, Hydrogen on silicene: Like or unlike graphene?, *Phys. Chem. Chem. Phys.* **18**, 15654 (2016).
- [41] R. B. Pontes, R. R. Mañano, R. da Silva, L. F. Cótica, R. H. Miwa, and J. E. Padilha, Electronic and optical properties of hydrogenated group-IV multilayer materials, *Phys. Chem. Chem. Phys.* **20**, 8112 (2018).
- [42] B. Huang, H.-X. Deng, H. Lee, M. Yoon, B. G. Sumpter, F. Liu, S. C. Smith, and S.-H. Wei, Exceptional Optoelectronic Properties of Hydrogenated Bilayer Silicene, *Phys. Rev. X* **4**, 021029 (2014).
- [43] B.-R. Wu, A DFT study for silicene quantum dots embedded in silicane: Controllable magnetism and tuneable band gap by hydrogen, *RSC Adv.* **9**, 32782 (2019).
- [44] J. Qiu, H. Fu, Y. Xu, A. I. Oreshkin, T. Shao, H. Li, S. Meng, L. Chen, and K. Wu, Ordered and Reversible Hydrogenation of Silicene, *Phys. Rev. Lett.* **114**, 126101 (2015).
- [45] J. Qiu, Y. Fu, Y. Xu, Q. Zhou, S. Meng, H. Li, L. Chen, and K. Wu, From silicene to half-silicane by hydrogenation, *ACS Nano* **9**, 11192 (2015).
- [46] W. Wang, W. Olovsson, and R. I. G. Uhrberg, Band structure of hydrogenated silicene on Ag(111): Evidence for half-silicane, *Phys. Rev. B* **93**, 081406(R) (2016).
- [47] W. Wei, Y. Dai, and B. Huang, Hydrogenation of silicene on Ag(111) and formation of half-silicene, *J. Mater. Chem. A* **5**, 18128 (2017).
- [48] A. Molle, C. Grazianetti, L. Tao, D. Taneja, M. Hasibul Alam, and D. Akinwande, Silicene, silicene derivatives, and their device applications, *Chem. Soc. Rev.* **47**, 6370 (2018).
- [49] P. D. Taylor, D. A. Osborne, S. A. Tawfik, T. Morishita, and M. J. S. Spencer, Tuning the work function of the silicene/ 4×4 Ag(111) surface, *Phys. Chem. Chem. Phys.* **21**, 7165 (2019).
- [50] M. Houssa, A. Dimoulas, and A. Molle, Silicene: A review of recent experimental and theoretical investigations, *J. Phys.: Condens. Matter* **27**, 253002 (2015).
- [51] H. Jamgotchian, Y. Colignon, N. Hamzaoui, B. Ealet, J. Y. Hoarau, B. Aufray, and J. P. Bibérian, Growth of silicene layers on Ag(111): Unexpected effect of the substrate temperature, *J. Phys.: Condens. Matter* **24**, 172001 (2012).
- [52] H. Liu, N. Han, and J. Zhao, Temperature and coverage effects on the stability of epitaxial silicene on Ag(111) surfaces, *Appl. Surf. Sci.* **409**, 97 (2017).
- [53] W. Li, S. Sheng, J. Chen, P. Cheng, L. Chen, and K. Wu, Ordered chlorinated monolayer silicene structures, *Phys. Rev. B* **93**, 155410 (2016).
- [54] P. Hohenberg and W. Kohn, Inhomogeneous electron gas, *Phys. Rev.* **136**, B864 (1964).
- [55] W. Kohn and L. J. Sham, Self-consistent equations including exchange and correlation effects, *Phys. Rev.* **140**, A1133 (1965).
- [56] J. P. Perdew, K. Burke, and M. Ernzerhof, Generalized Gradient Approximation Made Simple, *Phys. Rev. Lett.* **77**, 3865 (1996).
- [57] S. Grimme, Semiempirical GGA-type density functional constructed with a long-range dispersion correction, *J. Comput. Chem.* **27**, 1787 (2006).
- [58] P. Giannozzi *et al.*, QUANTUM ESPRESSO: A modular and open-source software project for quantum simulations of materials, *J. Phys.: Condens. Matter* **21**, 395502 (2009).

- [59] P. Giannozzi *et al.*, Advanced capabilities for materials modelling with Quantum ESPRESSO, *J. Phys.: Condens. Matter* **29**, 465901 (2017).
- [60] H. J. Monkhorst and J. D. Pack, Special points for Brillouin-zone integrations, *Phys. Rev. B* **13**, 5188 (1976).
- [61] A. Marini, C. Hogan, M. Grüning, and D. Varsano, yambo: An *ab initio* tool for excited state calculations, *Comput. Phys. Commun.* **180**, 1392 (2009).
- [62] G. Onida, L. Reining, and A. Rubio, Electronic excitations: Density-functional versus many-body Green's-function approaches, *Rev. Mod. Phys.* **74**, 601 (2002).
- [63] F. Bechstedt, L. Matthes, P. Gori, and O. Pulci, Infrared absorbance of silicene and germanene, *Appl. Phys. Lett.* **100**, 261906 (2012).
- [64] J. D. E. McIntyre and D. E. Aspnes, Differential reflection spectroscopy of very thin surface films, *Surf. Sci.* **24**, 417 (1971).
- [65] H. U. Yang, J. D'Archangel, M. L. Sundheimer, E. Tucker, G. D. Boreman, and M. B. Raschke, Optical dielectric function of silver, *Phys. Rev. B* **91**, 235137 (2015).
- [66] See Supplemental Material at <http://link.aps.org/supplemental/10.1103/PhysRevB.101.195413> for a discussion of Löwdin charges, electronic and optical properties of freestanding layers and clean Ag(111), as well as further details for the optical properties of functionalized silicene phases adsorbed on Ag(111).
- [67] P.-O. Löwdin, On the non-orthogonality problem connected with the use of atomic wave functions in the theory of molecules and crystals, *J. Chem. Phys.* **18**, 365 (1950).

Supplemental Material for Coverage-dependent electronic and optical properties of H or F passivated Si/Ag(111) from first-principles

A. Ugolotti* and G. P. Brivio

Materials Science Department, Università degli Studi di Milano-Bicocca, via Cozzi 55, 20125, Milano, Italy

Guido Fratesi

*ETSF and Dipartimento di Fisica “Aldo Pontremoli”,
Università degli Studi di Milano, via Celoria 16, 20133, Milano, Italy*

(Dated: April 15, 2020)

I. LÖWDIN CHARGES

In Table I are reported the electronic charge differences obtained as differences of the Löwdin partitioning between the adsorbed and clean/free-standing(FS) cases, namely $\Delta n = n_{\text{tot}} - n_{\text{Ag-clean}} - n_{\text{SiX-FS}}$. We remark that charge partitioning procedures may become misleading in the case where charge rearrangements mostly occur in the regions between atoms: as an example, for silicene both Si and Ag atoms are lowered in density in their immediate proximity, that is gained by the intermediate region; nevertheless, our Löwdin analysis attributes 0.41 e per unit cell more to Si. The case of silicane is even more significant in this respect: here, H atoms of the bottom layer are located within the regions where density accumulates, hence, they are attributed 2.09 e per unit cell (0.3 e each), despite their role is to weaken the interaction and the charge rearrangement in comparison to half-silicane. Therefore, the table with Löwdin charges is provided for completeness only but is not discussed further.

* a.ugolotti@campus.unimib.it

on Ag(111)	Si	hSiH	SiH	hSiF	SiF
Δn_{SiX}	0.4	0.4	1.8	0.2	-0.2
Δn_{Si}	0.4	0.2	-0.3	0.3	0.1
Δn_{X_u}	-	0.2	0.0	-0.1	-0.1
Δn_{X_d}	-	-	2.1	-	-0.2

Table I. Electronic number differences Δn for the different systems, expressed in electrons per cell, as obtained through Löwdin analysis for silicene (Si), half-silicene (hSiH), silicane (SiH), half-fluoro-silicane (hSiF) and fluoro-silicane (SiF) on Ag(111). X_u/X_d labels the H or F passivating atoms adsorbed on the upper/lower face of the silicene sheet.

II. FS ELECTRONIC STRUCTURE

We report in Fig. S1 the reference band structure and density of states (DOS) for the clean Ag(111) surface, within the $2\sqrt{3} \times 2\sqrt{3}R30^\circ$ supercell, and the FS silicene and its hydrogenated and fluorinated phases, in the $\sqrt{7} \times \sqrt{7}$ lattice. The projection on H or F atomic orbitals is shown as well. For half-silicene and half-fluoro-silicene we impose the regular chair-like configurations, such as those obtained in the presence of the Ag slab that are the focus of current investigation (keeping in mind that this may not be the more stable arrangement of adatoms without the substrate). The qualitative behavior computed for FS cases is very similar same, as a band gap of ≈ 2 eV can be observed, with the presence of hybrid Si-H/Si-F states around Fermi energy. As the coverage increases, the position of such states changes: for H adatoms the intraband states move far away from the valence band maximum (VBM), whereas for F adatoms they participate to the VBM.

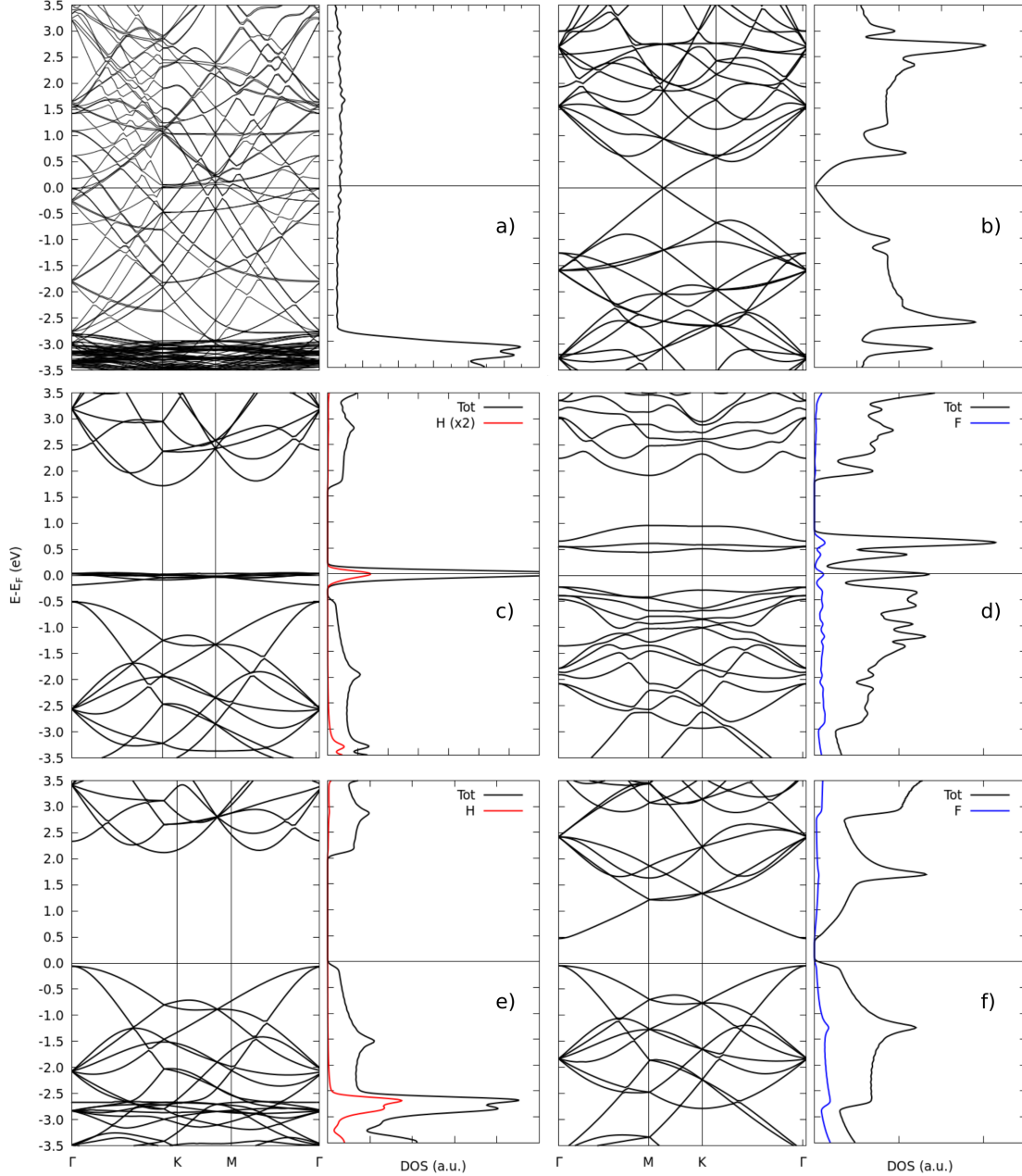


Figure 1. Band structure and DOS for a) clean Ag(111), FS b) silicene, c) half-silicane, d) half-fluoro-silicane, e) silicane and f) fluoro-silicane. All the plots refer to the $2\sqrt{3} \times 2\sqrt{3}R30^\circ$ (Ag) or $\sqrt{7} \times \sqrt{7}$ (silicene) phase. The projection on H/F atomic orbitals is reported with red/blue lines.

III. OPTICAL PROPERTIES OF THE ISOLATED SYSTEMS

The absorbance spectra are collected in Fig. S2 for the isolated clean surface and FS overlayers. The spectral intensity $S(E, \omega)$, see Eq. 2 in the main text, is reported as

well; such a quantity is proportional to the magnitude of the excitation dipoles for selected transition energies ω . It allows to interpret the origin within the electronic structure of the features in the absorbance spectrum by comparing the peaks in $S(E, \omega)$ with the density of states DOS(E).

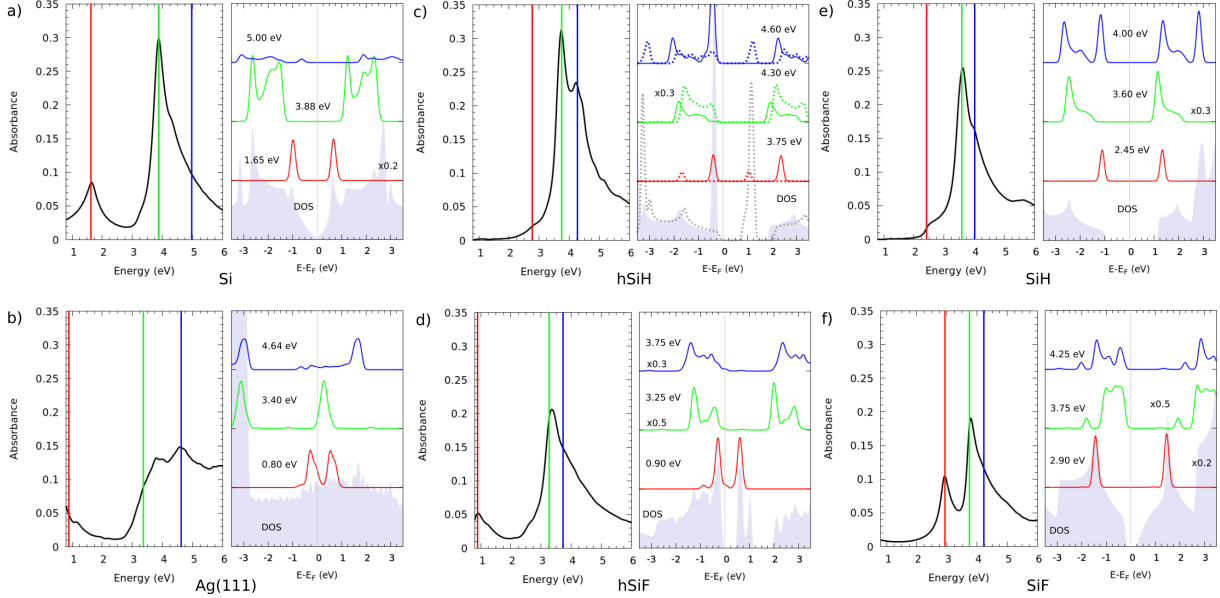


Figure 2. Absorbance spectra of a) Ag (bulk and clean slab) and free standing b) silicene, c) half-silicane, d) half-fluoro-silicane, e) silicane, f) fluoro-silicane. On the right side, the corresponding weighted distribution of the spectral intensities $S(E, \omega)$ along the density of states is reported for various transition energies ω . The DOS of each system is shown at the bottom as gray areas. The dashed lines represent the spin minority carriers in the spin-dependent calculations. All the plots refer to the $\sqrt{7} \times \sqrt{7}/2\sqrt{3} \times 2\sqrt{3}R30^\circ$ Ag(111) or silicene (and functionalized silicene) phases.

The features in the absorption spectrum can be correlated to the electronic structure via the joint bands; for FS silicene, for example, the peak at 1.65 eV in the former is explained in Ref. [C] to be the result of a Van Hove singularity, namely a saddle point along the surface of the joint bands. To try addressing systematically such features, we defined a \mathbf{k} -resolved spectral intensity $S(\mathbf{k}, \omega)$, which expresses the sum of the transition dipole moment, at every \mathbf{k} -point, on all valence-conduction pairs the energy of which is close enough to contribute to the selected transition ω . Its expression reads:

$$S(\mathbf{k}, \omega) = \int_{\omega-\sigma}^{\omega+\sigma} d\omega' \sum_{v\mathbf{k}, c\mathbf{k}} W_{v\mathbf{k}} W_{c\mathbf{k}} |\langle c\mathbf{k} | \hat{\mathbf{r}} | v\mathbf{k} \rangle|^2 \delta(\epsilon_{c\mathbf{k}} - \omega') \quad (1)$$

where $\epsilon_{cv\mathbf{k}} = \epsilon_{c\mathbf{k}} - \epsilon_{v\mathbf{k}}$ and σ is a broadening parameter (here $\sigma=0.05$ eV).

The pattern in the k -resolved spectral intensity should reflect the shape of the three-dimensional joint bands when intersecting with the plane at fixed energy ω . Therefore, a saddle point in the joint bands should form a cross-like shape and a minimum or maximum point should result in a circular pattern. The results of this approach for the FS silicene phases and clean Ag surface are reported in Fig. S3. We focus first on FS silicene as a verification of our approach; there, the aforementioned 1.65 eV peak can be indeed attributed to a Van Hove singularity at the high-symmetry M points in the reciprocal space. The apparent loss of symmetry and equivalence of the M points observed here is the result of the polarization of the perturbation along a specific axis, here x . For passivated phases of FS silicene, the absorption peaks are not related to high-symmetry points only. For example, in half-silicene and fluoro-half-silicene, the k -resolved spectral intensity for the higher-energy peaks, ≈ 4.30 and ≈ 3.25 eV respectively, does not show any pattern we could identify, suggesting us that the transitions take place from broader regions of the reciprocal space, with lower intensities. For clean Ag, the transitions are related to electronic excitations at the Γ point involving the edge of the d band.

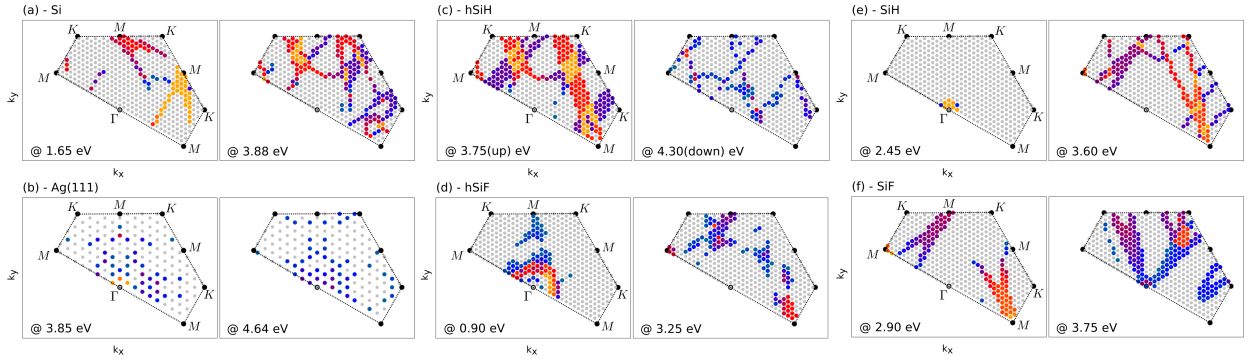


Figure 3. k -resolved spectral intensities, for different transition energies, of FS silicene (a), clean Ag(111) (b), FS half-silicene (c), FS silicene (d), FS half-fluoro-silicene (e) and FS fluoro-silicene (f).

In Fig. S4 we report the reflectivity spectrum of bulk Ag, calculated using Fresnel's laws through the dielectric function, as the reference for the differential spectroscopy. On passing, we notice that the theoretical results available from literature for silicene/Ag(111), for example in Refs. [A,E], are based on the LDA functional. Our PBE results improve upon such approximation; indeed, we obtain a better representation of the shape of the dip in

the spectra at around 3 eV, although such drop of reflectivity is red-shifted from the correct position. Such result is expected as both LDA and PBE neglect higher-order correlation effects between electrons, as discussed in Ref. [D].

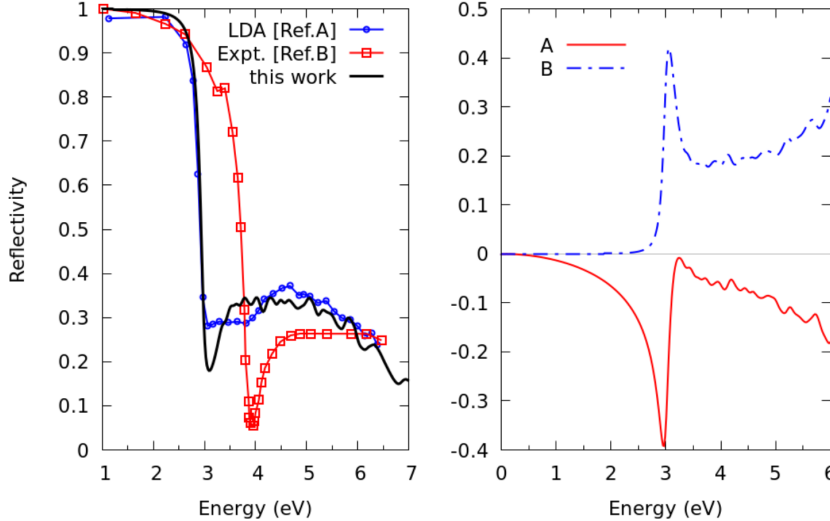


Figure 4. Left panel: comparison between the experimental reflectivity of bulk Ag (dotted red line) and the one calculated (through Fresnel’s equations) with different levels of DFT approximations: LDA (dotted blue line) or PBE (this work, black line). Right panel: plot of the auxiliary functions $F_{1,2}$ calculated from the bulk response function.

IV. OPTICAL PROPERTIES OF SILICENE PHASES ADSORBED ON Ag(111)

In Fig. S5 we report the comparison of coverage-dependent components, namely the Si-to-Si and Ag-to-Ag ones, along with total of the absorbance of silicene phases/Ag(111). The data is taken from Fig. 5 of the main text, but here is represented so as to compare a given contribution across the different phases.

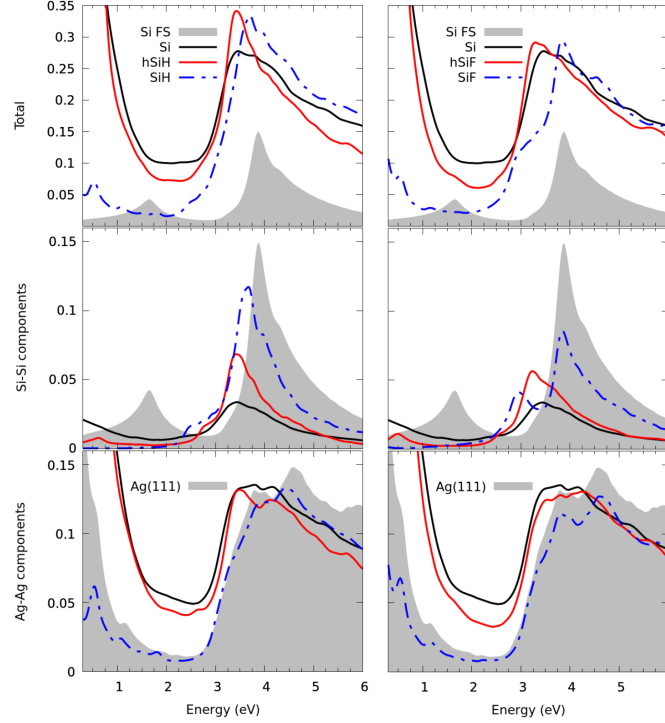


Figure 5. Components of the absorption spectra of silicene (Si, black line), half-silicene (hSiH, dot-dashed blue line), silicane (SiH, orange line), half-fluoro-silicane (hSiF) and fluoro-silicane (SiF) adsorbed on Ag(111). The spectra of FS silicene or clean slab are reported as gray areas.

V. REFERENCES

- (A) C. Hogan et al., “Optical properties of silicene, Si/Ag(111), and Si/Ag(110)”, Phys. Rev. B 97, (2018), 195407
- (B) H.U. Yang, J. D’Archangel, M.L. Sundheimer, E. Tucker, G.D. Boreman, M.B. Raschke, “Optical dielectric function of silver”, Phys. Rev. B 91, (2015), 235137
- (C) F. Bechstedt, L. Matthes, P. Gori, O. Pulci, “Infrared absorbance of silicene and germanene”, Appl. Phys. Lett. 100, (2012), 261906
- (D) A. Marini, R. Del Sole, and G. Onida, “First-principles calculation of the plasmon resonance and of the reflectance spectrum of silver in the GW approximation”, Phys. Rev. B 66 (2002), 115101
- (E) E. Cinquanta, G. Fratesi, S. dal Conte, C. Grazianetti, F. Scotognella, S. Stagira, C. Voizzi, G. Onida, A. Molle, “Optical response and ultrafast carrier dynamics of silicene-silver interface”, Phys. Rev. B 92, (2015), 165427